

Electroweak fragmentation functions for dark matter annihilation

Leila Ali Cavasonza^{1*}, Michael Krämer^{1,2†} and Mathieu Pellen^{1‡}

¹*Institute for Theoretical Particle Physics and Cosmology,
RWTH Aachen University, D-52056 Aachen, Germany*

²*SLAC National Accelerator Laboratory, Stanford University, Stanford, CA 94025, USA*

Abstract

Electroweak corrections can play a crucial role in dark matter annihilation. The emission of gauge bosons, in particular, leads to a secondary flux consisting of all Standard Model particles, and may be described by electroweak fragmentation functions. To assess the quality of the fragmentation function approximation to electroweak radiation in dark matter annihilation, we have calculated the flux of secondary particles from gauge-boson emission in models with Majorana fermion and vector dark matter, respectively. For both models, we have compared cross sections and energy spectra of positrons and antiprotons after propagation through the galactic halo in the fragmentation function approximation and in the full calculation. Fragmentation functions fail to describe the particle fluxes in the case of Majorana fermion annihilation into light fermions: the helicity suppression of the lowest-order cross section in such models cannot be lifted by the leading logarithmic contributions included in the fragmentation function approach. However, for other classes of models like vector dark matter, where the lowest-order cross section is not suppressed, electroweak fragmentation functions provide a simple, model-independent and accurate description of secondary particle fluxes.

*E-mail: cavasonza@physik.rwth-aachen.de

†E-mail: mkraemer@physik.rwth-aachen.de

‡E-mail: pellen@physik.rwth-aachen.de

Contents

1	Introduction	2
2	Electroweak corrections	3
2.1	The fragmentation function approach	3
3	Majorana fermion and vector dark matter	5
3.1	A supersymmetric model with Majorana fermion dark matter	5
3.2	A universal extra dimension model with vector dark matter	6
4	The secondary flux after propagation	10
4.1	Comparison and results	11
5	Conclusions	12

1 Introduction

The existence of dark matter [1] provides strong evidence for physics beyond the Standard Model (SM). A leading candidate for dark matter are weakly interacting massive particles, which may be produced at colliders or detected through direct and indirect detection experiments. In indirect detection, in particular, one searches for dark matter annihilation products, including antimatter particles like positrons and antiprotons, which propagate through the galactic halo and which can be detected in astrophysical experiments at the earth.

Electroweak (EW) corrections may be important for dark matter annihilation for two reasons [2, 3, 4, 5, 6, 7, 8, 9, 10, 11, 12, 13, 14, 15, 16, 17, 18, 19, 20, 21, 22, 23, 24]. First, the radiation of a vector boson can lift the helicity suppression of cross sections for Majorana fermion dark matter annihilating into light fermions [13, 14, 15, 16, 25, 26, 27, 28, 29]. Moreover, the emission and decay of electroweak gauge bosons from the primary annihilation products alter the spectrum and composition of the secondary flux. In particular, the gauge boson decay will lead to a secondary flux which includes all stable SM particles (e^+ , e^- , ν , $\bar{\nu}$, γ , p , \bar{p}), irrespective of the model-specific composition of the primary annihilation products.

Many models provide dark matter candidates with masses in the TeV-range, see *e.g.* Ref. [1, 30, 31, 32]. For such heavy dark matter, soft and collinear electroweak gauge boson emission from the relativistic final-state particles is enhanced by Sudakov logarithms $\ln^2(M_{\text{DM}}^2/M_{\text{EW}}^2)$ [33, 34, 35], where M_{DM} and M_{EW} are the mass of the dark matter candidate and of the electroweak gauge boson, respectively. The leading logarithmic contributions to the annihilation cross section can be described in a model-independent way by electroweak fragmentation functions [12, 36, 37], where improved splitting functions are introduced in order to take into account the masses of the emitted gauge bosons.

The purpose of the present article is to examine the quality of the fragmentation function approximation. To this end we have compared the predictions obtained for the secondary flux after propagation using the fragmentation function approximation against those obtained from an exact calculation. To perform the comparison we have chosen two specific dark matter models, a simplified version of the minimal supersymmetric model (MSSM) [30, 38] with neutralino dark matter, and a model with universal extra dimensions (UED) where the first Kaluza-Klein excitation of the photon provides a dark matter candidate [39, 40]. Both models are generic for the annihilation of Majorana fermion and vector dark matter, respectively. To assess the quality of the fragmentation function approach we focus on the particular case where the dark matter particles annihilate at lowest order into electron-positron pairs only. We show that the fragmentation function approach reproduces well the exact result in the case of UED with vector dark matter, while the approximation does not work for the MSSM with Majorana fermion annihilation into electron-positron pairs. This is due to the fact that the annihilation of Majorana fermions into a light lepton pair is helicity suppressed and that the emission of soft and collinear gauge bosons from the final-state particles, included in the fragmentation function approximation, is not sufficient to lift this helicity suppression [16]. Hence, the fragmentation function approximation provides a simple and model-independent way to obtain realistic predictions for dark matter indirect detection for those models where the annihilation cross section is not suppressed at the lowest order.

This article is organised as follows: in Section 2 we briefly review the fragmentation function approximation to electroweak radiation. In Section 3 we present the calculation of EW gauge boson emission in two specific models with Majorana fermion and vector dark matter, respectively, and compare the fragmentation function approximation against the exact result for the primary flux. In Section 4 we perform the comparison for the secondary flux after propagation through the galactic halo. We conclude in Section 5.

2 Electroweak corrections

Electroweak corrections in the context of dark matter annihilation have been widely discussed in the literature [2, 3, 4, 5, 6, 7, 8, 9, 10, 11, 12, 13, 14, 15, 16, 17, 18, 19, 20, 21, 22]. Therefore we only summarize the main ideas and describe the fragmentation function approach to describe electroweak gauge boson emissions.

2.1 The fragmentation function approach

We assume heavy dark matter *i.e.* $M_{\text{DM}} \gg M_{\text{EW}}$, which annihilates into electron-positron pairs only. The radiation of W and Z bosons off the high energy final-state leptons is enhanced by logarithms of the form $\ln(M_{\text{DM}}^2/M_{\text{EW}}^2)$ and $\ln^2(M_{\text{DM}}^2/M_{\text{EW}}^2)$ corresponding to collinear and soft/collinear emission, respectively. No such enhancement exists for radiation off the non-relativistic initial-state dark matter particles, or radiation off intermediate particles. Thus, in the limit $M_{\text{DM}} \gg M_{\text{EW}}$ the electroweak gauge boson emission is dominated by soft and collinear final-state radiation, which is independent of the specific dark matter model or the form of the annihilation cross section.

We are interested in the energy spectrum of a given SM final state $f \in \{e^\pm, \gamma, p, \bar{p}, \nu, \bar{\nu}\}$, resulting from the annihilation process $\text{DM DM} \rightarrow e^+e^- + (Z \rightarrow f)$, including the decay of the Z boson and the fragmentation and hadronisation of the decay products, see Fig 1.¹

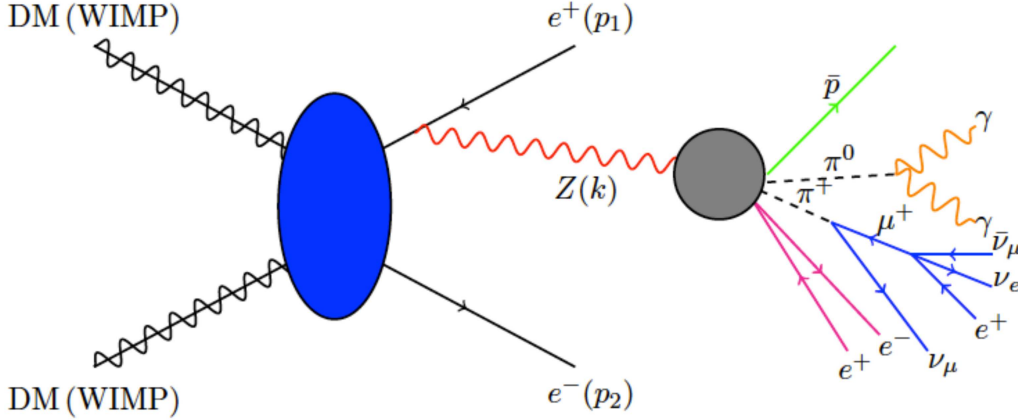


Figure 1: Generic annihilation process of DM into an electron-positron pair plus Z radiation, with Z decay, fragmentation and hadronisation.

The energy spectrum is given by

$$\frac{dN_f}{dx} = \frac{1}{\langle \sigma v_{\text{cm}} \rangle} \frac{d\langle \sigma v_{\text{cm}} \rangle}{dx}, \quad (1)$$

with $x = 2E_f/\sqrt{s}$ and $\langle \sigma v_{\text{cm}} \rangle$ the thermally averaged cross section for the process $\text{DM DM} \rightarrow e^+e^- (Z \rightarrow f)$. The centre-of-mass energy is $\sqrt{s} = 2M_{\text{DM}}/\sqrt{1-v_{\text{cm}}^2}$, and E_f denotes the energy of the final state SM particle of type f . By v_{cm} we denote the velocity of the dark matter particle in the centre-of-mass frame. More specifically, as the dark matter particles are non-relativistic, we have $x \simeq E_f/M_{\text{DM}}$. In contrast to some conventions in the literature, the energy spectrum, Eq. (1), is normalised to one, $\int dx dN_f/dx = 1$.

The logarithmically enhanced contributions to the emission of an electroweak boson can be described by fragmentation functions, D^{EW} , that obey evolution equations similar to the

¹For the sake of simplicity, we will focus only on the radiation of Z bosons in the following.

DGLAP equations [36, 37]. Within this formalism, the energy spectrum of a SM particle f is given by [12]

$$\frac{dN_f}{d\ln x}(M_{\text{DM}}, x) = \sum_J \int_x^1 dz D_{I \rightarrow J}^{\text{EW}}(z) \frac{dN_{J \rightarrow f}}{d\ln x} \left(zM_{\text{DM}}, \frac{x}{z} \right), \quad (2)$$

where I denotes the final state of the $(2 \rightarrow 2)$ annihilation process, *i.e.* an electron-positron pair in the case at hand. The summation in J includes the final state particles after the radiation of an EW gauge boson. In our case, $J \in \{e^+, e^-, Z\}$. The fragmentation functions $D_{I \rightarrow J}^{\text{EW}}(z)$ describe the probability that a particle I turns into a particle J , with a fraction z of the energy of the emitting particle, via the emission of a EW boson. Clearly at the lowest order we have $D_{I \rightarrow J}^{\text{EW}}(z) = \delta_{IJ}\delta(1-z)$. The further decay, fragmentation and hadronisation of the primary annihilation products, $J \rightarrow f$, can be described by standard Monte Carlo event generators.

The fragmentation functions $D_{I \rightarrow J}^{\text{EW}}(z)$ can be obtained by computing the partonic splitting functions. They differ from those of QCD or QED as the emitted EW gauge bosons are massive.² For our purposes, we need the splitting functions of a massless fermion (F) splitting into a massless fermion and a massive vector particle (V):

$$P_{F \rightarrow F} = \frac{1+x^2}{1-x} L(1-x), \quad (3a)$$

$$P_{F \rightarrow V} = \frac{1+(1-x)^2}{x} L(x), \quad (3b)$$

with

$$L(x) = \ln \frac{sx^2}{4m_Z^2} + 2 \ln \left(1 + \sqrt{1 - \frac{4m_Z^2}{sx^2}} \right). \quad (4)$$

The corresponding fragmentation functions are

$$D_{F \rightarrow F} = \frac{\alpha_2}{2\pi \cos^2 \theta_w} g_f^2 P_{F \rightarrow F}, \quad (5a)$$

$$D_{F \rightarrow V} = \frac{\alpha_2}{2\pi \cos^2 \theta_w} g_f^2 P_{F \rightarrow V}, \quad (5b)$$

where m_Z is the mass of the emitted Z boson, α_2 the $\text{SU}(2)$ coupling and θ_w the weak angle. The factor $g_f = T_3^f - \sin^2 \theta_w Q_f$ accounts for the coupling of the fermions to the Z boson, where T_3^f and Q_f are the isospin and the charge of the fermion, in our case e_L^\pm or e_R^\pm . The function L , Eq. (4), respects the correct kinematic limits and vanishes below threshold for $x < 2m_Z/\sqrt{s}$. Note that the fragmentation functions depend on the chirality of the fermion through the coupling g_f , so that one should sum over $e_L^+ e_L^-$ and $e_R^+ e_R^-$ pairs to obtain the annihilation cross section.

For the implementation of the fragmentation function approach in our Monte Carlo program, we use a Sudakov parametrisation of the phase space [12] to produce events according to the fragmentation function distributions. This is required only because we use a parton shower program to evolve the final state and it needs four momenta as input. Note that for observables at the annihilation point such as cross sections or distributions, like those in Figs. 3 and 5, Eq. (2) would be enough to determine the quantities of interest. The four-momentum of the initial state is denoted by

$$S^\mu = (2E, 0, 0, 0), \quad (6)$$

where $E = M_{\text{DM}}/\sqrt{1-v_{\text{cm}}^2}$. The momentum of the electron/positron that radiates the Z boson can be parametrised as

$$p_1 = \left(E \left(1 - x + \frac{k_t^2}{4E^2(1-x)} \right), -k_t, 0, E \left(1 - x - \frac{k_t^2}{4E^2(1-x)} \right) \right), \text{ with } k_t \ll E, \quad (7)$$

²For a more extended discussion and a complete listing of the EW splitting functions see Ref. [12].

where x corresponds to the fraction of energy carried away by the emitted Z boson. The four-momentum of the emitted Z boson takes the form

$$k_Z = \left(E \left(x + \frac{k_t^2 + m_Z^2}{4E^2 x} \right), k_t, 0, E \left(x - \frac{k_t^2 + m_Z^2}{4E^2 x} \right) \right). \quad (8)$$

Finally, the four-momentum of the electron/positron which does not radiate is

$$p_2 = (E(1 - R(1 - x, k_t)), 0, 0, -E(1 - R(1 - x, k_t))), \quad (9)$$

with

$$R(x, k_t) = \frac{k_t^2}{4E^2 x} + \frac{k_t^2 + m_Z^2}{4E^2(1 - x)}. \quad (10)$$

This parametrisation ensures the conservation of the four-momentum.

3 Majorana fermion and vector dark matter

In order to quantify the accuracy of the fragmentation function approximation, we have calculated dark matter annihilation into an e^+e^- -pair plus a Z boson, $\text{DM DM} \rightarrow e^+e^-Z$, in the minimal supersymmetric model (MSSM) with neutralino dark matter and in a model with universal extra dimensions (UED), where the dark matter is provided by the first Kaluza-Klein excitation of the photon. For both models, we have compared the energy spectrum of the Z boson within the fragmentation function approximation with the exact calculation of the $(2 \rightarrow 3)$ process, including the radiation of a Z boson from the intermediate t - and u -channel particles. In both cases, we have chosen the intermediate particle to be degenerate in mass with the dark matter particle. This choice, on the one hand, reduces the number of model parameters. On the other hand, because of an on-shell enhancement of the intermediate propagator for small electron/positron energies, the case of equal masses results in a spectrum which is most strongly peaked towards the maximal Z -boson energy. A priori, one would thus expect that the fragmentation function approach is less likely to reproduce the full calculation. We have used FEYNARTS and FORMCALC [41, 42, 43] for the MSSM calculation and CALCHEP [44, 45] for UED, and checked our results against MADGRAPH 5 [46].

The flux of the annihilation products is determined by the thermally averaged cross section, $\langle \sigma v_{\text{cm}} \rangle$, which can be expanded in powers of the dark matter velocity [47]:

$$\langle \sigma v_{\text{cm}} \rangle = a + bv_{\text{cm}}^2 + \mathcal{O}(v_{\text{cm}}^4). \quad (11)$$

Given that $v_{\text{cm}}^2 \approx 10^{-6}$ for the annihilation of dark matter in the halo, we only kept the first term of the expansion.

3.1 A supersymmetric model with Majorana fermion dark matter

As a specific model with Majorana fermion dark matter we have considered the MSSM and calculated the annihilation of neutralinos into an electron-positron pair, $\tilde{\chi}_0 \tilde{\chi}_0 \rightarrow e^+e^-$. We consider a pure bino, which does not couple to a Z boson, so that the annihilation proceeds through the exchange of selectrons in the t - and u -channel only. To derive analytic results, we have furthermore assumed that there is no neutralino and selectron mixing, and that the masses of the left- and right-chiral selectrons are degenerate. Without mixing, the vertices drastically simplify to $-ie\sqrt{2}P_L/(2\cos\theta_w)$ for the left-chiral selectron, \tilde{e}_L , and $ie\sqrt{2}P_R/\cos\theta_w$ for the right-chiral selectron, \tilde{e}_R , respectively [48, 49]. The Feynman diagrams for this process are displayed in Fig. 2. We have reproduced the result for the matrix element squared obtained in [50] and performed a low-velocity expansion of the Mandelstam variables to obtain the thermally averaged

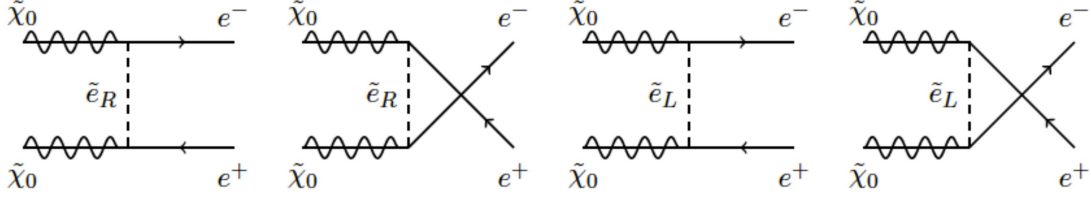


Figure 2: Lowest order contributions to neutralino annihilation into an electron-positron pair.

cross section [51, 52]. Retaining only the first coefficient of this expansion *i.e.* the zeroth order in the velocity, we obtain

$$\langle\sigma v_{\text{cm}}\rangle = \frac{\alpha^2 25\pi m_e^2 \sqrt{M_{\text{DM}}^2 - m_e^2}}{16M_{\text{DM}} \cos^4 \theta_w (M_{\text{DM}}^2 + m_e^2 - m_e^2)^2}, \quad (12)$$

where m_e and $m_{\tilde{e}} = m_{\tilde{e}_L} = m_{\tilde{e}_R}$ are the mass of the electron and of the selectrons, respectively, and α is the QED coupling. In the following we will always set $m_{\tilde{e}} = M_{\text{DM}}$ for simplicity. Note that because of the well-known helicity suppression [25, 26] due to the Majorana nature of the neutralino the cross section vanishes in the limit of zero electron mass $m_e \rightarrow 0$.

The $(2 \rightarrow 3)$ tree-level process, $\tilde{\chi}_0 \tilde{\chi}_0 \rightarrow e^+ e^- Z$, is finite, and we do not include virtual corrections as we are mainly interested in the shape of the secondary flux induced by the Z -boson decay. The helicity suppression of the $(2 \rightarrow 2)$ process, Eq. (12), is lifted by Z -boson radiation only if the emission from both the final- and intermediate state particles, *i.e.* from the electron-positron pair and from the t - and u -channel selectron, is included [16]. The fragmentation function approximation which only includes soft/collinear radiation off the electron/positron pair is thus expected not to work in this particular case. This can be seen explicitly from the s -wave contribution to the neutralino annihilation cross section, $\tilde{\chi}_0 \tilde{\chi}_0 \rightarrow e^+ e^- Z$, obtained in Ref. [16]:

$$\frac{dN_Z}{dx} = \frac{(1-x)}{(2-x)^2} \left[\frac{(1-x)}{(2-x)} \ln(1-x) + x \frac{(1-x)^2 + 1}{4(1-x)} \right], \quad (13)$$

where x is the energy fraction of the emitted Z boson and the mass of the electron is assumed to be zero. In Fig. 3 we compare the Z energy distribution of the full $(2 \rightarrow 3)$ calculation for bino annihilation into an electron-positron pair plus a Z boson with the fragmentation function approximation

$$\left. \frac{d\sigma_{(\text{DM DM} \rightarrow e^+ e^- Z)}}{dx} \right|_{\text{ff}} = 2 \left(\sigma_{(\text{DM DM} \rightarrow e_L^+ e_L^-)} D_{e_L \rightarrow Z} + \sigma_{(\text{DM DM} \rightarrow e_R^+ e_R^-)} D_{e_R \rightarrow Z} \right). \quad (14)$$

It is manifest from Fig. 3 that the fragmentation function approximation does not describe the energy distribution of the full $(2 \rightarrow 3)$ process. In general, the fragmentation function approach is not supposed to work if the lowest-order cross section is helicity suppressed, as in the case of Majorana fermion annihilation into light fermions. Moreover, since the splitting functions are convoluted with the $2 \rightarrow 2$ cross section, the $2 \rightarrow 3$ cross section obtained from the fragmentation function approach would be zero in the case of massless electron/positron.

3.2 A universal extra dimension model with vector dark matter

We now discuss a model with vector dark matter, where the lowest-order annihilation cross section to electron-positron pairs is not helicity suppressed. Specifically, we consider a model with universal extra dimensions where the first Kaluza-Klein excitation of the $U(1)_Y$ hypercharge

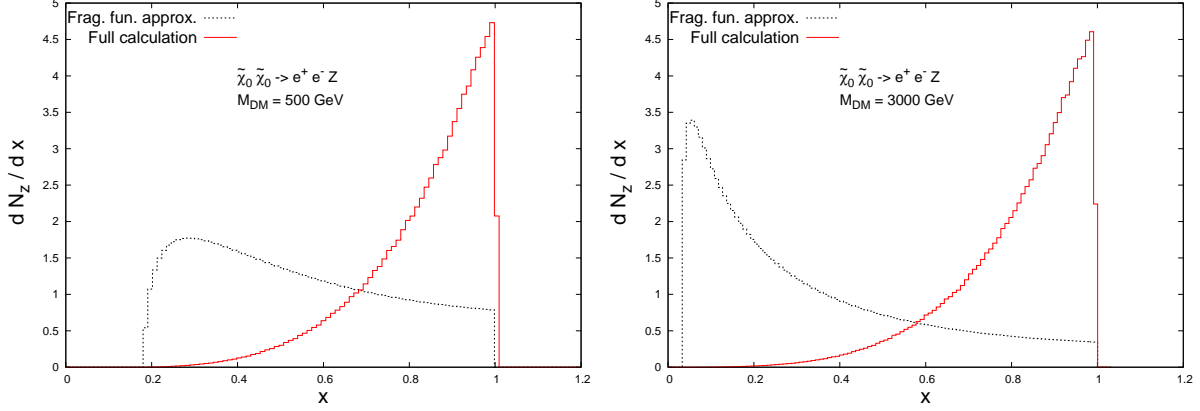


Figure 3: Z -boson energy spectrum dN_Z/dx , Eq. (1), for the annihilation of Majorana fermion dark matter into an electron-positron pair plus a Z boson in supersymmetry. (See the main text for the definition of the model.) Shown is the exact calculation (red, solid line) and the fragmentation function approximation (blue, dotted line) for $M_{\text{DM}} = 500$ and 3000 GeV.

gauge field, $B^{(1)}$, provides a dark matter candidate. The Feynman diagrams for the leading-order annihilation process, $B^{(1)}B^{(1)} \rightarrow e^+e^-$, mediated by t - and u -channel exchange of the first Kaluza-Klein excitation of the electron, $e_{L,R}^{(1)}$, are displayed in Fig. 4. For completeness

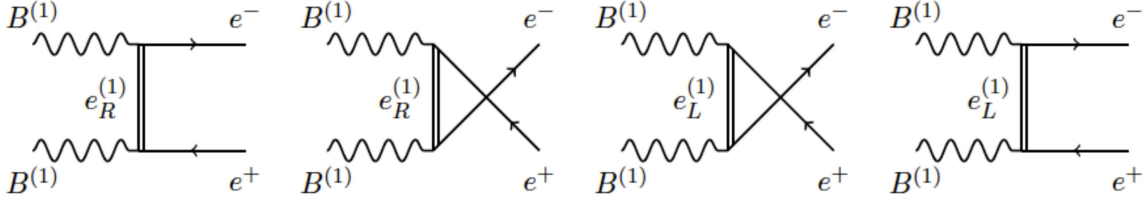


Figure 4: Lowest order contributions to Kaluza-Klein photon annihilation into an electron-positron pair.

we give the s -wave contribution of the thermally averaged annihilation cross section at leading-order [40, 53]:

$$\langle \sigma v_{\text{cm}} \rangle = \frac{(|g_L|^4 + |g_R|^4)}{576 M_{\text{DM}}^2 \pi}, \quad (15)$$

where $g_{L/R} = g_1 Y_{L/R}$ and the hypercharges for left- and right-handed electrons are $Y_L = -1$ and $Y_R = -2$, respectively. For simplicity, and to derive compact analytic expressions, we assume that all Kaluza-Klein particles are mass degenerate. From Eq. (15) it is clear that the process $B^{(1)}B^{(1)} \rightarrow e^+e^-$ is not helicity suppressed.

The emission of a Z boson in the $(2 \rightarrow 3)$ process $B^{(1)}B^{(1)} \rightarrow e^+e^-Z$ constitutes a genuine higher-order correction of $\mathcal{O}(\alpha \ln^2(M_{\text{DM}}^2/m_Z^2))$, and is thus significantly suppressed with respect to the lowest order cross section presented in Eq. (15), see Table 1. The prediction for the $(2 \rightarrow 3)$ process $B^{(1)}B^{(1)} \rightarrow e^+e^-Z$ in the fragmentation function approximation includes the logarithmically enhanced contributions $\propto \ln^{(1,2)}(M_{\text{DM}}^2/m_Z^2)$ only, and is thus expected to become more and more accurate with increasing dark matter mass. This is borne out by the explicit numerical comparison shown in Table 1. While the fragmentation function approximation underestimates the cross section by about a factor 3 for $M_{\text{DM}} = 150$ GeV, at $M_{\text{DM}} = 500$ GeV it already reproduces the normalisation of the full calculation within 10% accuracy.

The energy distributions of the emitted Z boson, dN_Z/dx , is shown in Fig. 5 for different masses of the dark matter particle. One can see that the fragmentation function approximation

M_{DM} [GeV]	$\langle\sigma v\rangle_{B^{(1)}B^{(1)}\rightarrow e^+e^-}$ [pb]	$\langle\sigma v\rangle_{B^{(1)}B^{(1)}\rightarrow e^+e^-Z}$ [pb]	$\langle\sigma v\rangle_{B^{(1)}B^{(1)}\rightarrow e^+e^-Z} _{\text{ff}}$ [pb]
150	2.642	4.583×10^{-3}	1.459×10^{-3}
300	0.6604	2.078×10^{-3}	1.597×10^{-3}
500	0.2378	1.202×10^{-3}	1.104×10^{-3}
1000	5.944×10^{-2}	5.362×10^{-4}	5.282×10^{-4}
3000	6.605×10^{-3}	1.221×10^{-4}	1.227×10^{-4}

Table 1: Thermally averaged cross section $\langle\sigma v\rangle$ for the annihilation of vector dark matter into an electron-positron pair, and with the radiation of a Z boson, in a universal extra dimension model. (See the main text for the definition of the model.). Shown are the lowest-order cross section, the exact cross section including Z -boson radiation, and the fragmentation function approximation to Z -boson radiation, for different masses of the dark matter particle. We have used $\sin^2\theta_w = 0.23113$ and $\alpha = 1/128$.

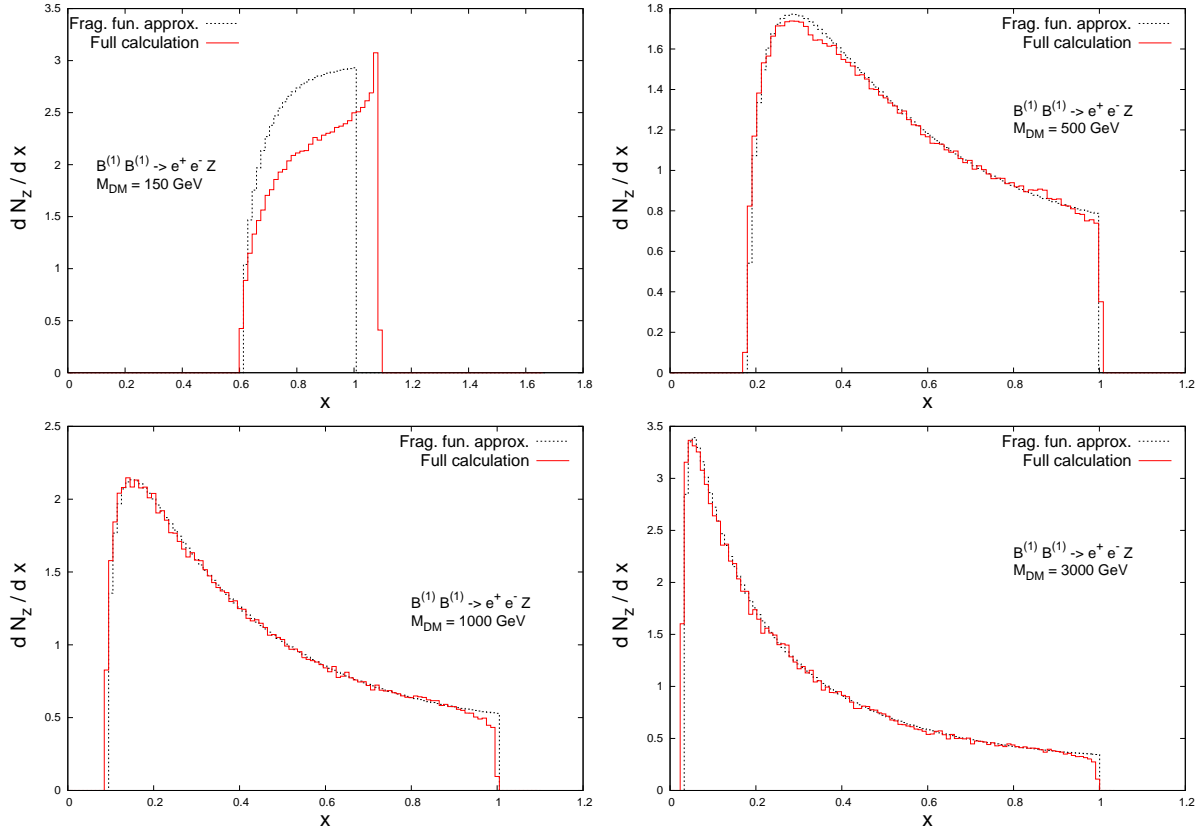


Figure 5: Z -boson energy spectrum dN_Z/dx , Eq. (1), for the annihilation of vector dark matter into an electron-positron pair plus a Z boson in a universal extra dimension model. (See the main text for the definition of the model.) Shown is the exact calculation (red, solid line) and the fragmentation function approximation (blue, dotted line) for $M_{\text{DM}} = 150, 500, 1000$ and 3000 GeV.

provides a very accurate description of the shape of the energy distributions for heavy dark matter with $M_{\text{DM}}/m_Z \gtrsim 5$.

The quality of the fragmentation function approximation can be deduced from the analytical expression that we have obtained for the exact $(2 \rightarrow 3)$ process $B^{(1)}B^{(1)} \rightarrow e_L^+e_L^-Z$. Integrating over the angles and considering the centre of mass of the annihilating particles, the differential cross section can be written as

$$vd\sigma = \frac{|\mathcal{M}|^2}{256\pi^3} dx_1 dx_2, \quad (16)$$

where $|\mathcal{M}|^2$ is the matrix element squared and x_1 and x_2 parametrise the energies of the final-state particles. In particular

$$k^0 = (1 - x_2)\sqrt{s}/2, \quad (17)$$

$$p_1^0 = x_1\sqrt{s}/2, \quad (18)$$

$$p_2^0 = (1 - x_1 + x_2)\sqrt{s}/2, \quad (19)$$

with the four momenta k, p_1 and p_2 corresponding to the Z boson, the positron and the electron, respectively. The integration limits of the phase space for the variable x_1 are

$$x_- \leq x_1 \leq x_+, \quad (20)$$

with

$$x_{\pm} = \frac{1 + x_2}{2} \pm \sqrt{\frac{(1 - x_2)^2}{4} - \frac{m_Z^2}{s}}. \quad (21)$$

For x_2 the integration boundaries are

$$-\frac{m_Z^2}{s} \leq x_2 \leq 1 - 2\frac{m_Z}{\sqrt{s}}. \quad (22)$$

Expanding in the velocity and integrating over x_1 , Eq. (16) becomes

$$\frac{d\langle\sigma v\rangle}{dx_2} = \frac{\alpha}{2304 M_{\text{DM}}^2 \pi^2} \frac{(1 - 2\sin^2\theta_w)^2}{\sin^2\theta_w \cos^2\theta_w} |g_L|^4 F(x_2), \quad (23)$$

The function F is defined as

$$F(x_2) = \left(A \ln\left(\frac{\bar{x}_+}{\bar{x}_-}\right) + B + C \ln\left(\frac{\bar{x}_+ - 2}{\bar{x}_- - 2}\right) \right), \quad (24)$$

with $\bar{x}_{\pm} = 1 - x_2 \pm \sqrt{(1 - x_2)^2 - m_Z^2/M_{\text{DM}}^2}$ and coefficients A, B and C given by

$$\begin{aligned} A &= -\frac{1}{8M_{\text{DM}}^6} \frac{1}{x_2(x_2 - 1)} \left(m_Z^6 + M_{\text{DM}}^2 m_Z^4 (4 + 5x_2) \right. \\ &\quad \left. + 4M_{\text{DM}}^4 m_Z^2 (1 + 3x_2 + 2x_2^2) + 8M_{\text{DM}}^6 (x_2 + x_2^3) \right), \\ B &= -\sqrt{(1 - x_2)^2 - \frac{m_Z^2}{M_{\text{DM}}^2}} + \frac{1}{16M_{\text{DM}}^6} \frac{1}{(1 + x_2)^2} \sqrt{(1 - x_2)^2 - \frac{m_Z^2}{M_{\text{DM}}^2}} \frac{1}{x_2 + \frac{m_Z^2}{4M_{\text{DM}}^2}} \left(2m_Z^6 \right. \\ &\quad \left. + 2M_{\text{DM}}^2 m_Z^4 (2 + 9x_2) + 12M_{\text{DM}}^6 x_2 (5 + 8x_2 + 5x_2^2) + 5M_{\text{DM}}^4 m_Z^2 (3 + 8x_2 + 11x_2^2) \right), \\ C &= \frac{1}{8M_{\text{DM}}^6} \left(M_{\text{DM}}^2 m_Z^4 (4 + 9x_2 - 4x_2^2 + 5x_2^3) + 8M_{\text{DM}}^6 x_2 (1 + 4x_2 + 9x_2^2 + 4x_2^3 + x_2^4) \right. \\ &\quad \left. + m_Z^6 (1 + x_2^2) + M_{\text{DM}}^4 m_Z^2 (4 + 25x_2 + 36x_2^2 - 7x_2^3 + 8x_2^4) \right) \frac{1}{x_2(1 + x_2)^3}. \end{aligned} \quad (25)$$

Given the Born cross section (see Eq. (15)), Eq. (23) can be recast in the form

$$\frac{d\langle\sigma v\rangle}{dx_2} = 2\langle\sigma v\rangle_{\text{Born}} \frac{\alpha}{2\pi} \frac{g_f^2}{\sin^2\theta_w \cos^2\theta_w} F(x_2). \quad (26)$$

This is exactly the form expected within the fragmentation function approach, see Eqs. (3), (4) and (5). Indeed in the limit $m_Z \rightarrow 0$,

$$A \ln \left(\frac{\bar{x}_+}{\bar{x}_-} \right) \rightarrow \frac{1+x_2^2}{1-x_2} \left(\ln \left((1-x_2)^2 \frac{M_{\text{DM}}^2}{m_Z^2} \right) + 2 \ln(2) \right), \quad (27)$$

which is exactly Eqs. (3) and (4) in this limit.

For completeness we have computed the coefficients A , B and C for an intermediate mass m_i different from the dark matter mass in the limit $m_Z \rightarrow 0$. In this case they read

$$\begin{aligned} A &= \frac{4}{(1+w^2)^2} \frac{-1+4x_2-3x_2^2+2x_2^3+w^2(1-2x_2+3x_2^2)}{(1-x_2)(-1+w^2+2x_2)}, \\ B &= -\frac{1+w^2}{2}(1-x_2) + \frac{1}{8(1+w^2)} \frac{1}{(w^2+x_2)^2} \frac{(x_2-1)}{w^4-1+2x_2(1+w^2)} \\ &\quad \left(-3+w^{10}+w^8(-3+x_2)-14x_2-28x_2^2-20x_2^3+w^6(6-23x_2+6x_2^2-2x_2^3) \right. \\ &\quad \left. -w^4(2-7x_2+44x_2^2+2x_2^3)-w^2(-1+31x_2+30x_2^2+36x_2^3) \right) \\ C &= \frac{1}{(w^2+x_2)^3} \frac{1}{4(1+w^2)^2} \frac{1}{(-1+w^2+2x_2)} \left(3-w^{14}-3w^{12}(-1+x_2)+8x_2 \right. \\ &\quad -10x_2^2-20x_2^3-16x_2^4+32x_2^5-w^{10}(-9-31x_2-6x_2^2+2x_2^3) \\ &\quad -w^2(1-7x_2+14x_2^2+110x_2^3-148x_2^4)-w^4(11-21x_2+176x_2^2-308x_2^3-4x_2^4) \\ &\quad \left. -w^6(-9+102x_2-232x_2^2-96x_2^3+4x_2^4)-w^8(11-70x_2-90x_2^2-16x_2^3+4x_2^4) \right), \end{aligned} \quad (28)$$

with $w = m_i/m_{\text{DM}}$. Furthermore, in Eq. (24) $\ln \left(\frac{\bar{x}_+-2}{\bar{x}_--2} \right)$ has to be replaced by $\ln \left(\frac{\bar{x}_+-(1+w^2)}{\bar{x}_--(1+w^2)} \right)$.

4 The secondary flux after propagation

In this section we compare the positron and antiproton fluxes obtained with the fragmentation function approximation against the exact result after propagation through the galactic halo. We briefly explain how we obtain the energy spectra of the stable Standard Model particles at the production point and how we implement the propagation of positrons and antiprotons.

In order to obtain the primary³ stable SM particles we use PYTHIA 8 [54, 55, 56] to describe the Z boson decay, the evolution of its decay products (further decays and hadronisation) and the QCD and QED radiation. The fluxes produced by PYTHIA 8 are then propagated through the galactic halo to obtain predictions for positrons and antiprotons at the earth.

As we are not aiming at a detailed study of the different dark matter profiles, and the uncertainty due to propagation, we have chosen the Einasto model [57, 58] as a specific example:

$$\rho_{\text{Ein}}(r) = \rho_s \exp \left(-\frac{2}{\alpha} \left[\left(\frac{r}{r_s} \right)^\alpha - 1 \right] \right), \quad (29)$$

where $\alpha = 0.17$, $r_s = 28.44$ kpc and $\rho_s = 0.033$ GeV/cm³. These values correspond to a dark matter density $\rho_\odot = 0.3$ GeV/cm³ at the location of the sun ($r_\odot = 8.33$ kpc).

In order to calculate the flux of positrons/electrons at the location of the earth, we have used the Green function formalism [59]. The expression for the positron/electron flux after

³“Primary” denotes the particles at the production point, while “secondary” denotes the particles after propagation.

propagation is [59]

$$\frac{d\Phi_{e^\pm}}{dE}(\epsilon, r_\odot) = \frac{1}{4\pi} \frac{v_{e^\pm}}{b_T(\epsilon)} \frac{1}{2} \left(\frac{\rho_\odot}{M_{\text{DM}}} \right)^2 \langle \sigma v_{\text{cm}} \rangle_{\text{DM DM} \rightarrow \text{I}} \int_\epsilon^{M_{\text{DM}}} d\epsilon_s \frac{dN_{e^\pm}}{dE}(\epsilon_s) \mathcal{I}(\lambda_D(\epsilon, \epsilon_s)), \quad (30)$$

with

$$\frac{dN_{e^\pm}}{dE} = \frac{1}{\langle \sigma v_{\text{cm}} \rangle_{\text{DM DM} \rightarrow \text{I}}} \frac{d\langle \sigma v_{\text{cm}} \rangle_{\text{DM DM} \rightarrow \text{I}} \times BR_{\text{I} \rightarrow e^\pm}}{dE}, \quad (31)$$

with ϵ the energy expressed in GeV, $I \in \{e^+e^-, e^+e^-Z\}$ and v_{e^\pm} is the velocity of the electron. The energy spectrum is normalized to the total cross section. The normalisation of the flux is given by $b_T(\epsilon) = \epsilon^2/\tau_\odot$ where $\tau_\odot = \text{GeV}/b(1 \text{ GeV}, r_\odot) = 5.7 \times 10^{15} \text{ sec}$. The functions λ_D and \mathcal{I} are defined as

$$\lambda_D = \lambda_D(\epsilon, \epsilon_s) = \sqrt{4\mathcal{K}_0\tau_\odot(\epsilon^{\delta-1} - \epsilon_s^{\delta-1})/(1-\delta)} \quad (32)$$

and

$$\mathcal{I}(\lambda_D) = a_0 + a_1 \tanh\left(\frac{b_1 - \ell}{c_1}\right) \left[a_2 \exp\left(-\frac{(\ell - b_2)^2}{c_2}\right) + a_3 \right], \quad (33)$$

with $\ell = \log_{10}(\lambda_D/\text{kpc})$. The values of the astrophysical parameters \mathcal{K}_0 , δ , a_0 , a_1 , a_2 , a_3 , b_1 and b_2 are taken from Ref. [59] and correspond to the medium (MED) Einasto profile: $(a_0, a_1, a_2, a_3, b_1, b_2, c_1, c_2, \delta, \mathcal{K}_0) = (0.507, 0.345, 2.095, 1.469, 0.905, 0.741, 0.160, 0.063, 0.70, 0.0112)$.

The flux of antiprotons from dark matter annihilation at the earth is given by [59]

$$\frac{d\Phi_{\bar{p}}}{dK}(\epsilon, r_\odot) = \frac{1}{2} \frac{v_p}{4\pi} \left(\frac{\rho_\odot}{M_{\text{DM}}} \right)^2 R(K) \langle \sigma v_{\text{cm}} \rangle \frac{dN_{\bar{p}}}{dK}, \quad (34)$$

where $K = E - m_p$ and m_p are the kinetic energy and the mass of the proton respectively. The function R is defined as

$$\log_{10} [R(K)/\text{Myr}] = a_0 + a_1\kappa + a_2\kappa^2 + a_3\kappa^3 + a_4\kappa^4 + a_5\kappa^5, \quad (35)$$

with $\kappa = \log_{10}(K/\text{GeV})$ and the coefficients again taken from Ref. [59]: $(a_0, a_1, a_2, a_3, a_4, a_5) = (1.8804, 0.5813, -0.2960, -0.0502, 0.0271, -0.0027)$.

4.1 Comparison and results

We consider the spectra for positrons and antiprotons from the annihilation of vector dark matter in the universal extra dimension model after propagation through the galactic halo. We compare the results from the full $(2 \rightarrow 3)$ calculation and the fragmentation function approximation. In Fig. 6 the positron spectra after parton shower and propagation are displayed. The fragmentation function approximation provides an accurate description of the positrons from the Z -boson decay. However, as the cross section of the $(2 \rightarrow 3)$ process is a genuine electroweak higher-order contribution of $\mathcal{O}(\alpha \ln^2(M_{\text{DM}}^2/m_Z^2))$, and thus highly suppressed by comparison to the leading-order annihilation, the amount of additional positrons is small compared to those produced in the $(2 \rightarrow 2)$ process. The small dip in the fragmentation function prediction at high energies is a remnant of the kinematics of the $2 \rightarrow 2$ process and is disappearing as M_{DM}/m_Z increases.

In our simple leptophilic model set-up, antiprotons are generated exclusively from Z -boson decay. As the fragmentation function provides a good approximation to the Z -boson spectrum of the exact calculation, the flux of antiprotons is also expected to be reproduced well. This is indeed born out by the explicit calculation presented in Fig. 7. We find that the exact $(2 \rightarrow 3)$ calculation and the fragmentation function approach agree within 10% for $M_{\text{DM}} \gtrsim 500 \text{ GeV}$.

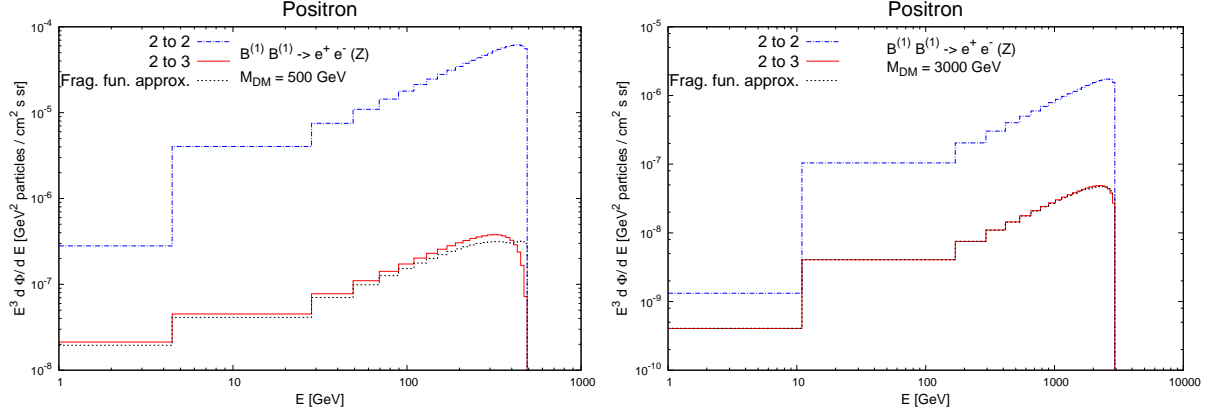


Figure 6: Positron flux $d\Phi/dE$, Eq. (30), after propagation through the galactic halo for the annihilation of vector dark matter into an electron-positron pair plus a Z boson in a universal extra dimension model. (See the main text for the definition of the model.) Shown is the lowest-order flux (blue, dashed line), the exact calculation of the flux from Z radiation (red, solid line) and the fragmentation function approximation (black, dotted line) for $M_{\text{DM}} = 500$ and 3000 GeV.

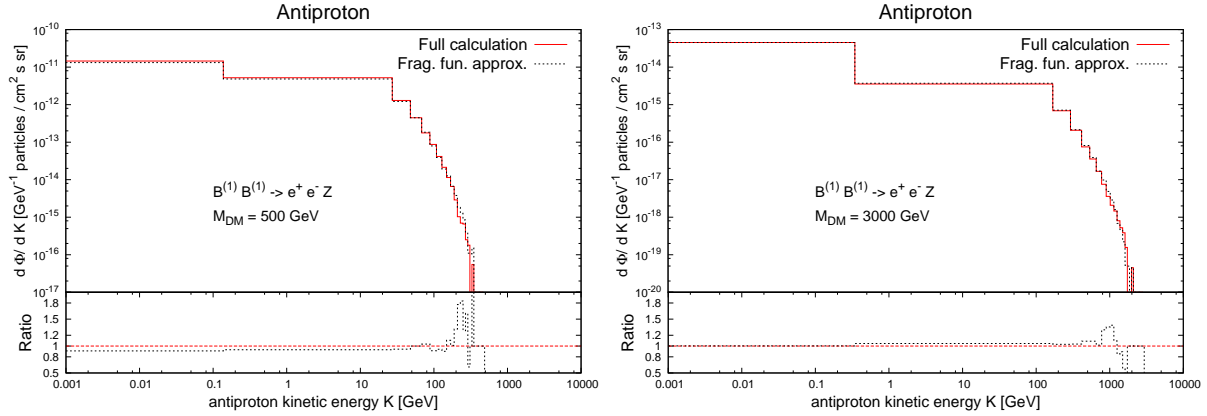


Figure 7: Antiproton flux $d\Phi/dK$, Eq. (34), after propagation through the galactic halo for the annihilation of vector dark matter into an electron-positron pair plus a Z boson in a universal extra dimension model. (See the main text for the definition of the model.) Shown is the exact calculation of the flux from Z radiation (red, solid line) and the fragmentation function approximation (black, dotted line) for $M_{\text{DM}} = 500$ and 3000 GeV.

5 Conclusions

The radiation of electroweak gauge bosons may be of crucial importance for dark matter annihilation. Vector boson emission lifts the helicity suppression of cross sections for Majorana fermion dark matter annihilating into light fermions, and it alters the spectrum and composition of the secondary flux. The decay of Z bosons, in particular, leads to a secondary flux which includes all stable SM particles, independent of the model-specific composition of the primary annihilation products.

For heavy dark matter, $M_{\text{DM}} \gg m_Z$, the emission of electroweak gauge bosons is enhanced by Sudakov logarithms $\ln^2(M_{\text{DM}}^2/m_Z^2)$. The leading logarithmic contributions from soft and collinear gauge boson emission can be described by electroweak fragmentation functions. We have quantified the quality of the fragmentation function approximation by comparing the fragmentation function prediction with the exact calculation for dark matter annihilation into an electron-positron pair plus a Z boson, $\text{DM} + \text{DM} \rightarrow e^+e^- + Z$. Specifically, we have investigated a supersymmetric model and a universal extra dimension model with Majorana fermion and vector dark matter, respectively. We provide predictions for the energy distribution of the Z

boson and the secondary flux of positrons and antiprotons after propagation through the galactic halo in both the fragmentation function approximation and the exact calculation of the $(2 \rightarrow 3)$ process.

We find that the fragmentation function approach fails for the supersymmetric model with Majorana fermion annihilation into electron-positron pairs. The emission of soft/collinear vector bosons, as included in the fragmentation function approximation, is not sufficient to lift the helicity suppression of the lowest-order annihilation cross section. For vector dark matter annihilation, on the other hand, the fragmentation function approach works very well and can describe the shape and normalisation of the secondary flux accurately. Specifically, we find that the particle fluxes obtained from the exact $(2 \rightarrow 3)$ calculation and the fragmentation function approach agree to better than 10% for $M_{\text{DM}} \approx 500 \text{ GeV}$ and to better than 2% for $M_{\text{DM}} \approx 1 \text{ TeV}$.

Thus, the fragmentation function approximation provides a simple and model-independent way to obtain realistic predictions for particle fluxes from dark matter annihilation for those models where the annihilation cross section is not suppressed at the lowest order.

Acknowledgement

We would like to thank Alexander Mück and Torbjörn Sjöstrand for useful discussions, Angéline Bieler for her collaboration at an early stage of this work, and Benedikt Marquardt for reading the manuscript. MK is grateful to SLAC and Stanford University for their hospitality. This work was supported by the Deutsche Forschungsgemeinschaft through the graduate school “Particle and Astroparticle Physics in the Light of the LHC” and through the collaborative research centre TTR9 “Computational Particle Physics”, and by the U.S. Department of Energy under contract DE-AC02-76SF00515.

References

- [1] Gianfranco Bertone, Dan Hooper, and Joseph Silk. Particle dark matter: Evidence, candidates and constraints. *Phys.Rept.*, 405:279–390, 2005.
- [2] Cyrille Barbot and Manuel Drees. Production of ultraenergetic cosmic rays through the decay of superheavy X particles. *Phys.Lett.*, B533:107–115, 2002.
- [3] V. Berezhinsky, M. Kachelriess, and S. Ostapchenko. Electroweak jet cascading in the decay of superheavy particles. *Phys.Rev.Lett.*, 89:171802, 2002.
- [4] Cyrille Barbot and Manuel Drees. Detailed analysis of the decay spectrum of a super heavy X particle. *Astropart.Phys.*, 20:5–44, 2003.
- [5] M. Kachelriess and P.D. Serpico. Model-independent dark matter annihilation bound from the diffuse γ ray flux. *Phys.Rev.*, D76:063516, 2007.
- [6] Nicole F. Bell, James B. Dent, Thomas D. Jacques, and Thomas J. Weiler. Electroweak Bremsstrahlung in Dark Matter Annihilation. *Phys.Rev.*, D78:083540, 2008.
- [7] James B. Dent, Robert J. Scherrer, and Thomas J. Weiler. Toward a Minimum Branching Fraction for Dark Matter Annihilation into Electromagnetic Final States. *Phys.Rev.*, D78:063509, 2008.
- [8] V. Barger, Y. Gao, Wai Yee Keung, and D. Marfatia. Generic dark matter signature for gamma-ray telescopes. *Phys.Rev.*, D80:063537, 2009.
- [9] Jean-Francois Fortin, Jessie Shelton, Scott Thomas, and Yue Zhao. Gamma Ray Spectra from Dark Matter Annihilation and Decay. 2009.
- [10] M. Kachelriess, P.D. Serpico, and M. Aa. Solberg. On the role of electroweak bremsstrahlung for indirect dark matter signatures. *Phys.Rev.*, D80:123533, 2009.
- [11] Paolo Ciafaloni and Alfredo Urbano. TeV scale Dark Matter and electroweak radiative corrections. *Phys.Rev.*, D82:043512, 2010.
- [12] Paolo Ciafaloni, Denis Comelli, Antonio Riotto, Filippo Sala, Alessandro Strumia, et al. Weak Corrections are Relevant for Dark Matter Indirect Detection. *JCAP*, 1103:019, 2011.
- [13] Nicole F. Bell, James B. Dent, Thomas D. Jacques, and Thomas J. Weiler. W/Z Bremsstrahlung as the Dominant Annihilation Channel for Dark Matter. *Phys.Rev.*, D83:013001, 2011.
- [14] Nicole F. Bell, James B. Dent, Thomas D. Jacques, and Thomas J. Weiler. Dark Matter Annihilation Signatures from Electroweak Bremsstrahlung. *Phys.Rev.*, D84:103517, 2011.
- [15] Nicole F. Bell, James B. Dent, Ahmad J. Galea, Thomas D. Jacques, Lawrence M. Krauss, et al. W/Z Bremsstrahlung as the Dominant Annihilation Channel for Dark Matter, Revisited. *Phys.Lett.*, B706:6–12, 2011.
- [16] Paolo Ciafaloni, Marco Cirelli, Denis Comelli, Andrea De Simone, Antonio Riotto, et al. On the Importance of Electroweak Corrections for Majorana Dark Matter Indirect Detection. *JCAP*, 1106:018, 2011.
- [17] Mathias Garny, Alejandro Ibarra, and Stefan Vogl. Antiproton constraints on dark matter annihilations from internal electroweak bremsstrahlung. *JCAP*, 1107:028, 2011.

- [18] Mathias Garny, Alejandro Ibarra, and Stefan Vogl. Dark matter annihilations into two light fermions and one gauge boson: General analysis and antiproton constraints. *JCAP*, 1204:033, 2012.
- [19] Paolo Ciafaloni, Denis Comelli, Andrea De Simone, Antonio Riotto, and Alfredo Urbano. Electroweak Bremsstrahlung for Wino-Like Dark Matter Annihilations. *JCAP*, 1206:016, 2012.
- [20] Nicole F. Bell, Amelia J. Brennan, and Thomas D. Jacques. Neutrino signals from electroweak bremsstrahlung in solar WIMP annihilation. *JCAP*, 1210:045, 2012.
- [21] Paolo Ciafaloni, Denis Comelli, Andrea De Simone, Enrico Morgante, Antonio Riotto, et al. The Role of Electroweak Corrections for the Dark Matter Relic Abundance. *JCAP*, 1310:031, 2013.
- [22] Torsten Bringmann and Francesca Calore. Significant Enhancement of Neutralino Dark Matter Annihilation from Electroweak Bremsstrahlung. *Phys.Rev.Lett.*, 112:071301, 2014.
- [23] Alejandro Ibarra, Maximilian Totzauer, and Sebastian Wild. Higher order dark matter annihilations in the Sun and implications for IceCube. *JCAP*, 1404:012, 2014.
- [24] Pietro Baratella, Marco Cirelli, Andi Hektor, Joosep Pata, Morten Piibeleht, et al. PPPC 4 DM ν : a Poor Particle Physicist Cookbook for Neutrinos from Dark Matter annihilations in the Sun. *JCAP*, 1403:053, 2014.
- [25] H. Goldberg. Constraint on the Photino Mass from Cosmology. *Phys.Rev.Lett.*, 50:1419, 1983.
- [26] H. Goldberg. Erratum: Constraint on the Photino Mass from Cosmology. *Phys. Rev. Lett.*, 103:099905, 2009.
- [27] Lars Bergstrom. Radiative Processes in Dark Matter Photino Annihilation. *Phys.Lett.*, B225:372, 1989.
- [28] Torsten Bringmann, Lars Bergstrom, and Joakim Edsjo. New Gamma-Ray Contributions to Supersymmetric Dark Matter Annihilation. *JHEP*, 0801:049, 2008.
- [29] Lars Bergstrom, Torsten Bringmann, and Joakim Edsjo. New Positron Spectral Features from Supersymmetric Dark Matter - a Way to Explain the PAMELA Data? *Phys.Rev.*, D78:103520, 2008.
- [30] Gerard Jungman, Marc Kamionkowski, and Kim Griest. Supersymmetric dark matter. *Phys.Rept.*, 267:195–373, 1996.
- [31] Matthew W. Cahill-Rowley, JoAnne L. Hewett, Ahmed Ismail, Michael E. Peskin, and Thomas G. Rizzo. pMSSM Benchmark Models for Snowmass 2013. 2013.
- [32] Matthew Cahill-Rowley, Randy Cotta, Alex Drlica-Wagner, Stefan Funk, JoAnne Hewett, et al. Complementarity of Dark Matter Searches in the pMSSM. 2014.
- [33] P. Ciafaloni and D. Comelli. Sudakov enhancement of electroweak corrections. *Phys.Lett.*, B446:278–284, 1999.
- [34] Johann H. Kuhn, A.A. Penin, and Vladimir A. Smirnov. Summing up subleading Sudakov logarithms. *Eur.Phys.J.*, C17:97–105, 2000.

- [35] Victor S. Fadin, L.N. Lipatov, Alan D. Martin, and M. Melles. Resummation of double logarithms in electroweak high-energy processes. *Phys.Rev.*, D61:094002, 2000.
- [36] Marcello Ciafaloni, Paolo Ciafaloni, and Denis Comelli. Towards collinear evolution equations in electroweak theory. *Phys.Rev.Lett.*, 88:102001, 2002.
- [37] Paolo Ciafaloni and Denis Comelli. Electroweak evolution equations. *JHEP*, 0511:022, 2005.
- [38] John R. Ellis, J.S. Hagelin, Dimitri V. Nanopoulos, Keith A. Olive, and M. Srednicki. Supersymmetric Relics from the Big Bang. *Nucl.Phys.*, B238:453–476, 1984.
- [39] Hsin-Chia Cheng, Jonathan L. Feng, and Konstantin T. Matchev. Kaluza-Klein dark matter. *Phys.Rev.Lett.*, 89:211301, 2002.
- [40] Geraldine Servant and Timothy M.P. Tait. Is the lightest Kaluza-Klein particle a viable dark matter candidate? *Nucl.Phys.*, B650:391–419, 2003.
- [41] Thomas Hahn. Generating Feynman diagrams and amplitudes with FeynArts 3. *Comput.Phys.Commun.*, 140:418–431, 2001.
- [42] Thomas Hahn and Christian Schappacher. The Implementation of the minimal supersymmetric standard model in FeynArts and FormCalc. *Comput.Phys.Commun.*, 143:54–68, 2002.
- [43] T. Hahn and M. Perez-Victoria. Automatized one loop calculations in four-dimensions and D-dimensions. *Comput.Phys.Commun.*, 118:153–165, 1999.
- [44] Alexander Belyaev, Neil D. Christensen, and Alexander Pukhov. CalcHEP 3.4 for collider physics within and beyond the Standard Model. *Comput.Phys.Commun.*, 184:1729–1769, 2013.
- [45] Asesh Krishna Datta, Kyoungchul Kong, and Konstantin T. Matchev. Minimal Universal Extra Dimensions in CalcHEP/CompHEP. *New J.Phys.*, 12:075017, 2010.
- [46] Johan Alwall, Michel Herquet, Fabio Maltoni, Olivier Mattelaer, and Tim Stelzer. MadGraph 5 : Going Beyond. *JHEP*, 1106:128, 2011.
- [47] Mark Srednicki, Richard Watkins, and Keith A. Olive. Calculations of Relic Densities in the Early Universe. *Nucl.Phys.*, B310:693, 1988.
- [48] Howard E. Haber and Gordon L. Kane. The Search for Supersymmetry: Probing Physics Beyond the Standard Model. *Phys.Rept.*, 117:75–263, 1985.
- [49] M. Drees, P. Roy, and R. Godbole. *Theory and Phenomenology of Sparticles: An Account of Four-dimensional N*. World Scientific, 2004.
- [50] Kim Griest. Cross-Sections, Relic Abundance and Detection Rates for Neutralino Dark Matter. *Phys.Rev.*, D38:2357, 1988.
- [51] James D. Wells. Annihilation cross-sections for relic densities in the low velocity limit. 1994.
- [52] Leszek Roszkowski. A Simple way of calculating cosmological relic density. *Phys.Rev.*, D50:4842–4845, 1994.

- [53] Kyoungchul Kong and Konstantin T. Matchev. Precise calculation of the relic density of Kaluza-Klein dark matter in universal extra dimensions. *JHEP*, 0601:038, 2006.
- [54] Torbjorn Sjostrand, Stephen Mrenna, and Peter Z. Skands. PYTHIA 6.4 Physics and Manual. *JHEP*, 0605:026, 2006.
- [55] Torbjorn Sjostrand, Stephen Mrenna, and Peter Z. Skands. A Brief Introduction to PYTHIA 8.1. *Comput.Phys.Commun.*, 178:852–867, 2008.
- [56] Torbjorn Sjostrand. PYTHIA 8 Status Report. pages 726–732, 2008.
- [57] Alister W. Graham, David Merritt, Ben Moore, Juerg Diemand, and Balsa Terzic. Empirical models for Dark Matter Halos. I. Nonparametric Construction of Density Profiles and Comparison with Parametric Models. *Astron.J.*, 132:2685–2700, 2006.
- [58] Julio F. Navarro, Aaron Ludlow, Volker Springel, Jie Wang, Mark Vogelsberger, et al. The Diversity and Similarity of Cold Dark Matter Halos. 2008.
- [59] Marco Cirelli, Gennaro Corcella, Andi Hektor, Gert Hutsi, Mario Kadastik, et al. PPPC 4 DM ID: A Poor Particle Physicist Cookbook for Dark Matter Indirect Detection. *JCAP*, 1103:051, 2011.